FIELD STUDIES OF SINGLE POINT IMPACT ON LIQUEFIABLE SOIL FOUNDATION OF HIGHWAY

Shen Zheng(沈正)[1], *Liu Zhibin*(刘志彬)[2], *Fang Lei*(方磊)[2], *Li Hanguang*(李汉光)[3]

(1. Department of Civil Engineering, Nanjing Institute of Technology, Nanjing, 211167, P. R. China;
2. Institue of Geotechnical Engineering, Southest University, Nanjing, 210096, P. R. China;
3. Xuzhou City Department of Transportation, Xuzhou, 221002, P. R. China)

Abstract: A highway in the floodplain of the Abandoned Yellow River in the north of Jiangsu Province is recently remediated to reduce liquefaction potential using the dynamic compaction(DC) method of densification of in-place soils. Firstly, the liquefaction potential of the soil at the project site is analysed according to the code of seismic design. Then the in-situ single point impact tests are performed on the liquefiable soil. Settlement of crater, excess pore pressure, ground heave and lateral deformation under DC impact are measured and analyzed. Subsequently, the standard penetration test (SPT) and cone penetration test (CPT) are used for investigating the compaction effectiveness. At last, the improvement effect of DC is discussed according to the technical specification of dynamic consolidation to ground treatment. The investigation results indicate that the DC technique is an effective way for remediating liquefiable soil in highway engineering practice.

Key words: dynamic compaction; single point impact; liquefaction; standard penetration test (SPT); improvement depth

CLC number: U416 **Document code**: A **Article ID**: 1005-1120(2013)04-0404-06

INTRODUCTION

Due to the many advantages of simple construction, reasonable economy and manifest reinforcing effect, dynamic compaction(DC) is widely applied to the foundation treatment of many projects. There are many case histories in soil improvement engineering. Miao[1] reported the relative increase in cone penetration test (CPT) values following DC as a function of time after DC. Zhang[2] used dynamic method to treat clayey silt soils. The method has been used for different types of civil engineering projects, including building structures, highways, airports, coal facilities, and dockyards[3-10]. Meanwhile, with the rapid pace of industrialization, highways are being designed and constructed in floodplains of abandoned Yellow River. Soils in floodplains often comprise saturated loose, fine sands and silts within the top 6—12 m of the ground surface. When situated in earthquake prone areas, these types of soils have significant liquefaction potential in the form of lateral spreading, sand boils, settlement, or cracking. Therefore, to reduce liquefaction potential, stabilization of the in-place soils is frequently required before highways are constructed on these types of soils. Liquefaction of saturated sand or silt and their remediation have been the topic of extensive research over the past decade, and through comparison with other methods, DC has been verified to be an effective method to reduce liquefaction potential of soil.

However, the remediation of liquefied soils is related to the characteristics of soils, so the corresponding remediation requirement must be put forward for different liquefied soils. In the

Foundation items: Supported by the National Youth Science Foundation of China (40802065); the Jiangsu Province Education Science Foundation (08KJD580004); the Innovation Research Foundation of Nanjing Institute of Technology (CKJ2011010).

Received date: 2011-11-13; **revision received date**: 2012-04-06

Corresponding author: Shen Zheng, Associate Professor, E-mail: sz751026@163.com.

project site, calyed silt and silt are widely distributed in the ground surface. Based on the liquefaction potential analyses at the site, the soils to depths of approximately 8 m from the ground surface have significant liquefaction potential. Considering the cost saving and completing project on time, DC is recommended to remediate the site. To investigate the effectiveness of DC for improving liquefiable silt soil foundation and determine and optimize the design and construction parameters of DC, the in-situ single point tamping tests involved of settlement of crater, excess pore pressure, ground heave, lateral deformation, the standard penetration test and cone penetration test are performed on the liquefied foundation.

1 PROJECT AND SITE DESCRIPTION

The proposed project site is located in Lianyungang-Xuzhou highway where is the floodplain of the abandoned Yellow River, in the province of Jiangsu, China. The ground surface at the time of construction is relatively flat and typical of alluvial plains, with an elevation change of less than 1 m, and the groundwater at the time of subsurface exploration is approximately 1.7 m below the ground surface. A total of eight borings are drilled as a part of the preliminary subsurface exploration. According to the geotechnical investigation, the soil layers at the site are shown in Table 1.

Table 1 Soil profile at dynamic compaction site

Soil layer	Soil name	Depth range/m	Colour	Nature water content/%	N-value	Plasticity index	Illustration
1	Clayed Silt, silt	0—4.5	Drab	27.6	2—5	8.5	Liquefaction
2	Clayed Silt, silt	4.5—7.6	Grey	30.8	3—8	11.6	Liquefaction
3	Silty clay	7.6—9.0	Grey	29.2	7—19	15.1	
4	Silty clay, silt fine sand	9.0—12.0	Drab	33.0	8—20	12.8	

2 LIQUEFACTION POTENTIAL OF SITE

There are several active earthquake source regions in the north of Jiangsu province, however, it is reasonable to assume that only the Tan Lu Seismic Zone (TLSZ) poses a threat in the Jiangsu province at this time. Based on the studies performed by China Seismological Bureau (CSB), a moment magnitude of 6.0 from TLSZ is used for a 10-year event in the Jiangsu province. The current seismic hazard maps developed by CSB for ground motions that have a 10% probability of being exceeded in 50 years show the peak ground acceleration (PGA) at the site is approximately 0.20 g. Fig. 1 presents the corrected results of standard penetration test (SPT) blows (N-value) of the test site and the number of blows required to reduce liquefaction potential at the site according to Chinese code for seismic design of highway engineering (JTG/T B02-01—2008). Based on the liquefaction potential analyses at the site, it is concluded that the existing soils to depths of approximately 6 m and 8 m from the ground surface have significant potential for liquefaction when the seismic intensity is separately 7 and 8 degree. These depths are consistent with the depths of saturated silty clays and silt encountered during subsurface exploration.

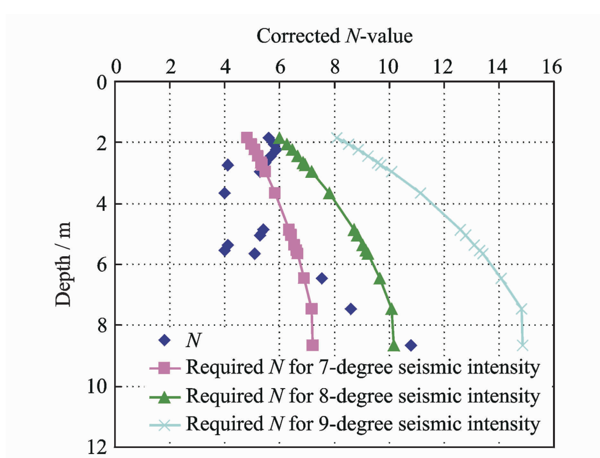

Fig. 1 SPT N-values showing liquefaction potential at the site and N-values required avoiding liquefaction potential

3 DESIGN AND TESTING OF DYNAMIC COMPACTION

Before the formal construction, the single point impact test is carried out. Due to the liquefied foundation, the detailed single point impact tests which include settlement of crater, pore water pressure, horizontal displacement, SPT, CPT and so on are performed especially for impact energy level 2000 kN • m. The impact energy level is respectively 1 500, 2 000 kN • m (the tamper weight is respectively 15, 20 t, and drop height is 10 m). Fig. 2 shows the layout of single impact point in the test zone. For the impact point (S_1) of impact energy level 1 500 kN • m, four observation sites (N_1, N_2, N_3, N_4) are set in the horizontal direction, whose distance from the impact point center is 2, 4, 6, and 8 m. For the impact point(S_2) of impact energy level 2 000 kN • m, also four observation sites (N_1, N_2, N_3, N_4) are set in the horizontal direction, whose distance from the impact point center is 2.4, 3.8, 5.7, and 7.2 m.

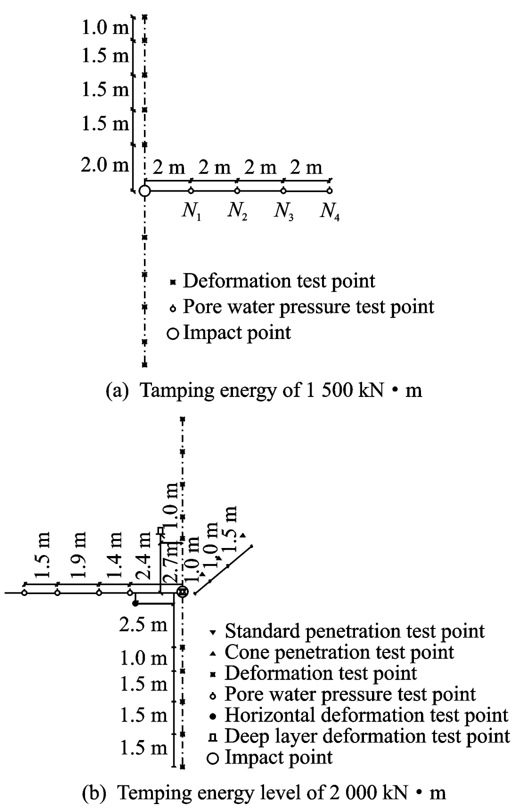

Fig. 2 Layout of impact points and test points under different impact energy of single compaction

4 SITE TESTING OF DYNAMIC COMPACTION

4.1 Testing of single point drops

4.1.1 Relationship between settlement and drops

It can be seen from Fig. 3, the settlement per drop gradually decreases for the first several drops when impact energy level is 2 000 kN • m, and the average settlement of the crater for the fourth drop is 20 cm. After four drops, the crater depth is 1.2 m, then the settlement of the crater increases suddenly with the seventh drop. This is likely to be due to the collapse of soil at the tamping pit wall after the sixth drop. Meanwhile, the settlement with the first four drops is 1.14 m when impact energy level is 1 500 kN • m, but for subsequent drops the settlements per drop is approximately 20 cm. Therefore, according to the relationship between crater depth and number of drops, it is concluded that the optimum number of drops is 5 when the impact energy level is 1 500 kN • m, whereas the optimum number of drops is 4 when the impact energy level is 2 000 kN • m, and it also illustrates the optimum number of drops decreases as the increase of tamper weight when drop height is unchanged.

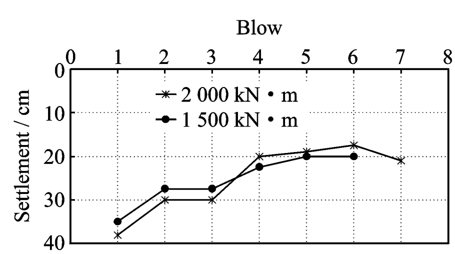

Fig. 3 Relationship between settlement and blows

4.1.2 Relationship between pore water pressure and drops

The pore water pressure of foundation corresponding to blow counts for the single point impact is given in Figs. 4—5. As the increase of blows, the pore water pressure grows up, and it shows larger rate of increase for the 1st blow than that of other blows. Meanwhile, the rate of increase in the shallower layer is faster than that of the deeper layer. For the single point impacts of impact energy level 1 500 kN • m, we find that the excess pore water pressures will be stable at 3, 5 and 7 m depth after the 5th blow, and the excess pore water pressure at 10 m depth is small. The phenomena illustrates that effective depth arrange of impact energy level 1 500 kN • m of DC arrives at 7 m. For the single point impacts of impact energy level 2 000 kN • m, we find that the excess pore water pressures will be stable at 3, 5, 7 m depth after the third blow, and the excess pore water pressure at 10 m depth is larger than that of impact energy level 1 500 kN • m. The phenomena illustrates that effective depth arrange of impact energy level 2 000 kN • m of DC will arrive at 8 m.

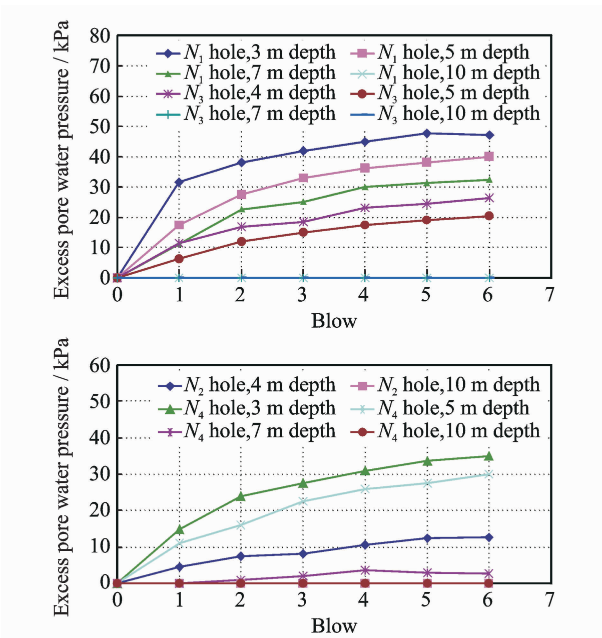

Fig. 4 Relationship between excess pore water pressure and blows for 1 500 kN • m impact energy

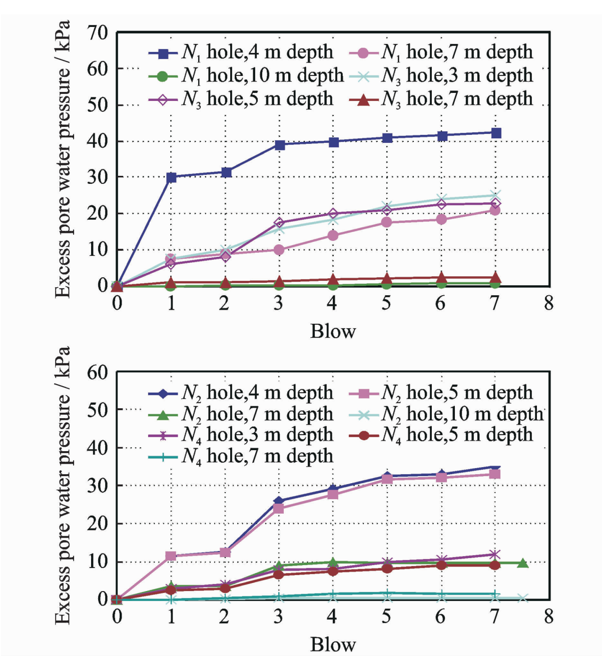

Fig. 5 Relationship between pore water pressure and blows for 2 000 kN • m impact energy

4.1.3 Relationship between excess pore water pressure and depth

It can be seen from Figs. 6-7 that the excess pore water pressure of foundation gradually decreases as the increase of depth in the process of tamping. For the single point impacts of impact energy level 1 500 kN • m, the excess pore water pressure of foundation gradually decreases when the depth is ranged from 3 m to 7 m for N_1 observation hole, then decreases suddenly when the depth is greater than 7 m. On the other hand, for N_2 observation hole the excess pore water pressure of foundation gradually decreases when the depth is ranged from 3 m to 5 m and from 7 m to 10 m, however decreases suddenly when the depth is ranged from 3 m to 5 m. This is likely to be due to the nearer distance from the impact point for N_1 observation hole. For N_3 and N_4 observation holes, the excess pore water pressure is very little when the depth is above 7 m.

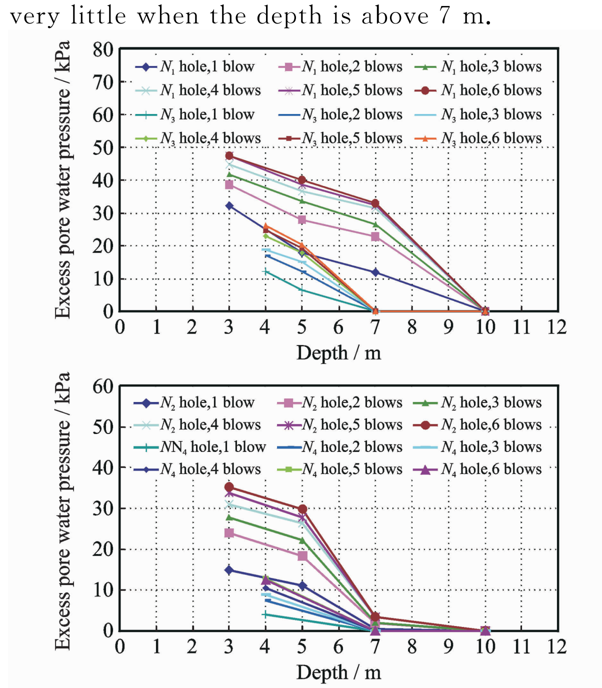

Fig. 6 Relationship between excess pore water pressure and depth for 1 500 kN • m impact energy

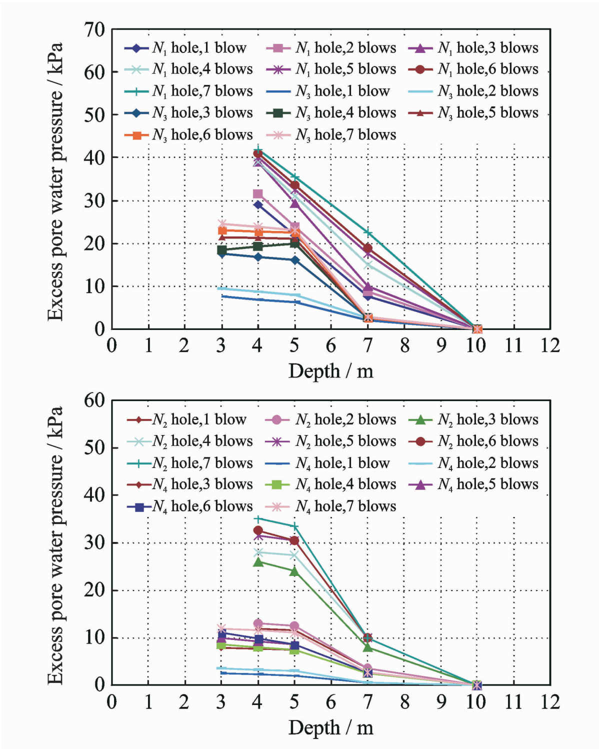

Fig. 7 Relationship between excess pore water pressure and depth for 2 000 kN • m impact energy

When impact energy level is 2 000 kN • m, the excess pore water pressure of foundation gradually decreases as the increase of depth in the process of tamping for N_1 hole, however, the excess static pore water pressure changes a little for N_2, N_3 and N_4 holes at the depth ranged from 3 m to 5 m, then decreases suddenly when the depth is ranged from 5 m to 7 m.

It is concluded that the influence depth of DC both is 8 m near the impact points and gently far from the impact point, and the influence depth is separately 6, 7 m when impact energy level is 1 500 kN • m and 2 000 kN • m.

4. 1. 4 Relationship between excess pore water pressure and horizontal distance

Fig. 8 illustrates that the excess pore water pressure of foundation gradually decreases with the growth of horizontal distance away from the impact point at the depth of 4 m for 1 500 kN • m and 2 000 kN • m impact energy. When the observation site is at the larger distance from the impact point center of 4 m and the monitoring position is at the depth of 4 m under the ground surface, the excess pore water pressure of foundation is very little. Moreover as the monitoring position is at the depth of 10 m under the ground surface, the excess pore water pressure of foundation is very little nearly 0. Generally speaking, the excess pore water pressure decreases faster in the deeper layer. The excess pore water pressure of foundation is nearly 0 when it is 7. 5—8 m away from impact point, which mainly conforms the test result of ground heave.

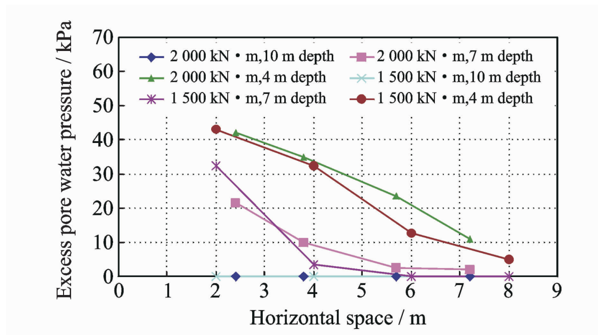

Fig. 8 Relationship between excess pore water pressure and horizontal space

4. 1. 5 Dissipation law of pore water pressure with time

It can be seen from Fig. 9 that the pore water pressure dissipates rapidly in the first ten minutes for 1 500 kN • m impact energy at the different observation holes and depth, which is attributed to good permeability of the soil. Subsequently, the pore water pressure dissipates more slowly than that of the first ten minutes especially from 50th minute to 110th minute except for N_4 observation hole which is monitored at the depth of 7 m under the ground surface. Finally, the pore water pressure dissipates over in the 140th minute. Generally, the shorter the time is, the further away from the tamping point is. It also can be seen from Fig. 10 that pore water pressure dissipates rapidly in the first ten minutes for 2 000 kN • m impact energy at the different observation holes which are monitored at 3—5 m depth under the ground surface, then dissipates slowly until a steady state is reached at the 155th minute, whereas the pore water pressure for N_3 and N_4 observation holes which are monitored at

7—10 m depth under the ground surface is very little and dissipates very slowly.

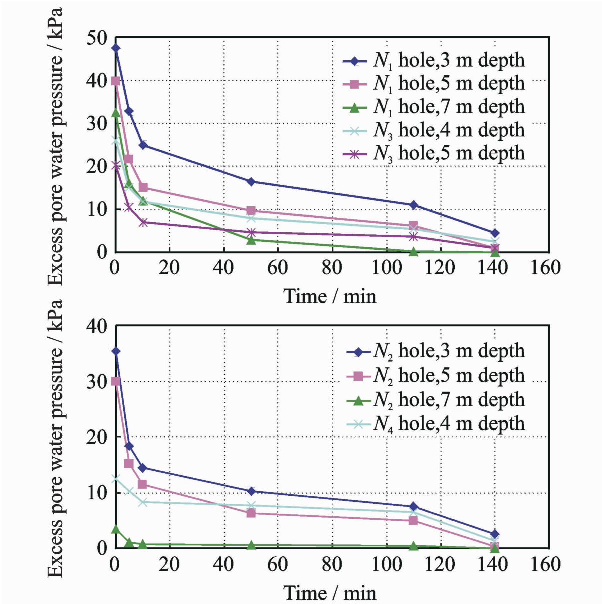

Fig. 9 Relationship between excess pore water pressure and time for 1 500 kN · m impact energy

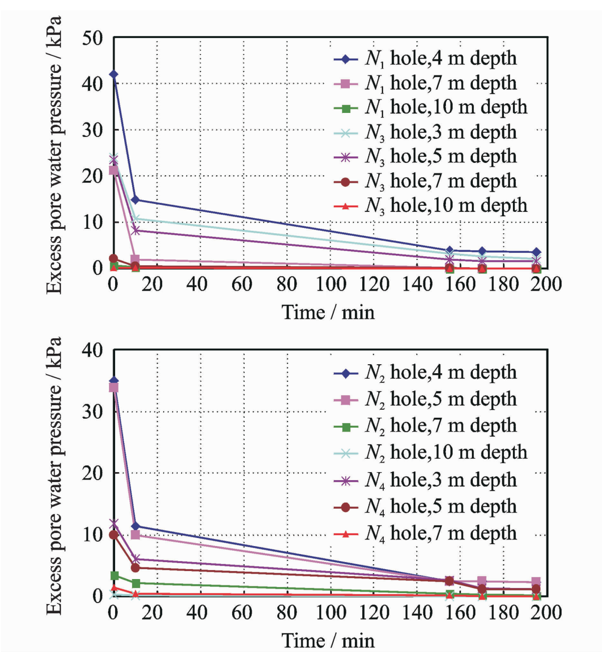

Fig. 10 Relationship between excess pore water pressure and time for 2 000 kN · m impact energy

4.1.6 Ground heave

The ground surface heaves around impact points are shown in Fig. 11. It can be seen that notable ground heave is observed with an impact energy level of 1 500 kN · m and 2 000 kN · m. Moreover, the ground heave gradually increases with the growth of blows, which is probably due to the increase of crater depth. At S_1, the maximum ground heave is 120 mm, and the radius of heave ranges from 7.0 m to 7.5 m. At S_2, the maximum ground heave is 86 mm, and the radius of heave is 8 m on the ground surface, which is attributed to the higher impact energy of S_2. In addition to S_2, the ground heave after the fifth blow is larger than that of the first fourth blows. Generally, the higher the impact energy level or the heavier the tamper weight is, the larger the radius of influence becomes.

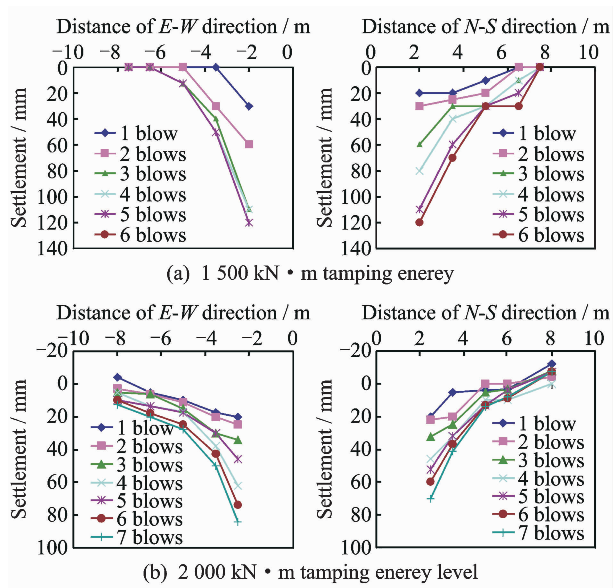

Fig. 11 Relationship between ground heave and horizontal space

4.1.7 Horizontal displacements

Test results of horizontal displacements for single point impacts of impact energy level 2 000 kN · m is given in Fig. 12. It can be seen from Fig. 12 that the effective depth arrange of DC arrives at 7 m, and the lateral displacement is 0. In addition, the lateral displacement is the largest in the depth of 1.2 m below the ground surface at the beginning of tamping time, and the lateral displacement is 65 mm in the depth of 1.2 m below the ground surface after the fourth blow. It can also be seen from Fig. 12 that the lateral displacement gradually decreases with the increase of depth. Moreover, the lateral displacement of ground surface grows rapidly after the fifth blow, whereas the lateral displacement of the deeper layer gently changes, which shows that the impact energy ends due to the ground surface deformation after five blows.

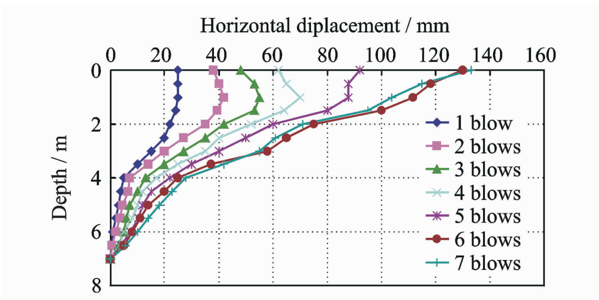

Fig. 12 Change of horizontal displacement with depth

4.2 Analysis on effectiveness of DC

In order to analyze the effectiveness of DC, SPT and CPT in situ testing method are used before and after DC. Due to the liquefied foundation of test zone and proper impact energy, the SPT and CPT tests are carried out in the test zone with 2 000 kN·m of impact energy. The test results are discussed below. Depths shown on all the figures presented are referenced to the original ground surface, i. e. ground surface before removal of surface soils.

4.2.1 Standard penetration test

Standard penetration test is a useful quick method for determining the relative stiffness and density of superficial deposits. The dynamic penetration test apparatus is equipped with a conventional probe head with a 51 mm diameter. The 63.5 kg hammer is dropped from the standard height of 760 mm and blow counts record every 100 mm to the required depth. The dynamic penetration is ended when three successive blow counts exceed 50, or when the probing rod rebounds. Standard penetration tests are conducted on the impact points, and two borings are drilled to depths of 12 m from the lowered ground surface in the 7th day after completion of single impact. Standard penetration test results (N-value) recorded during original subsurface exploration and after the single point impact are shown in Fig. 13.

From the data shown in Fig. 13, it is concluded that in general, the dynamic compaction improves the density of the existing silt deposit to approximate depths of 6 m and 7 m when the impact energy is separately 1 500 kN·m and 2 000 kN·m, and N-values in the surface soils and subsurface soils after DC for 1 500 kN·m and 2 000 kN·m of impact energy , to depths of 8 m are observed to be higher than the number of blows required to reduce the liquefaction potential when the seismic intensity is 7 degree. However, N-values after DC only for 2 000 kN·m tamping energy, to depths of 7 m are observed to be higher than the number of blows required to reduce the liquefaction potential for 8 degree seismic intensity. Due to 8 degree seismic fortification intensity for the project site, impact energy level 2 000 kN·m is recommended to remediate liquefiable silt soils.

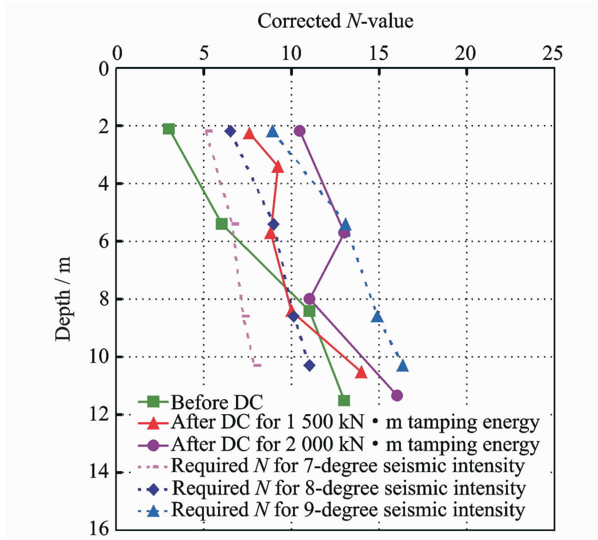

Fig. 13 SPT before and after DC for 1 500 and 2 000 kN·m of impact energy in test zone

4.2.2 Cone penetration test

CPT is becoming increasingly more popular as an in-situ test for site investigation and geotechnical design. This test is unequalled with respect to the delineation stratigraphy and the continuous rapid measurement of parameters like cone bearing, q_c, and sleeve friction, f_s. The procedure and equipment of the quasi-static electric CPT are easily standardized. The most significant advantages of CPT are simplicity, repeatability, accuracy and continuous record. A series of CPTs are performed before and after single point dynamic compaction in order to determine the depth of improvement. CPT results recorded during original subsurface exploration and after the single point impact are shown in Fig. 14.

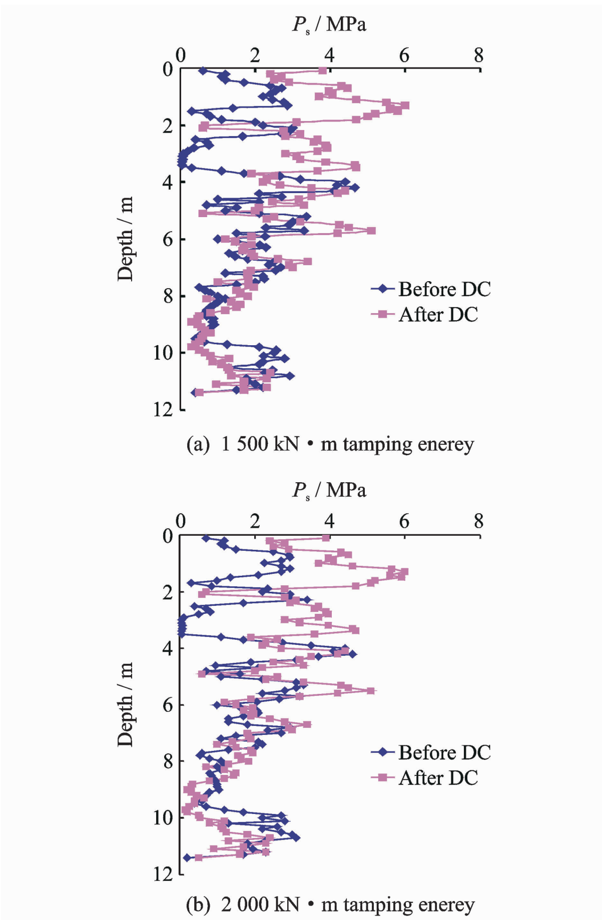

Fig. 14 CPT before and after DC for 1 500 kN • m and 2 000 kN • m of impact energy in test zone

It can be seen from Fig. 14 that the P_s values of CPT show the marked increase after DC compared with the values recorded before DC at the depth of 0—4 m, especially at the depth of 3—3. 5 m, where soft soil interbedding foundation is encountered. Then the P_s values are slightly larger than those recorded before DC at the depth of 4—7 m, while the P_s values vary gently (the measured depth > 7 m) compared with those measured before DC. Based on the measured values, it is concluded that in general, the in-place soils at depth above 4 m are well densified and the effective depth of the impact energy 1 500 kN • m and 2 000 kN • m in test zone is separately 6 m and 7 m. This is in agreement with the behavior of SPT conclusions.

4. 2. 3 Effective improvement depth of DC

According to the Chinese technical specification of dynamic consolidation to ground treatment (YSJ 209—92), the effective improvement depth is given as follows

$$H=\alpha\sqrt{hT}$$

where H is the effective improvement depth in meters, T the tamper weight in tons, h the tamper drop height in meters, and α the reduction factor of effective improvement depth. According to the equation, the heavier tamper weight is, the larger H is, which is conformed to the foregoing analysis. Due to clayed silt, according to Table 1 of the above specification, α is changed among 0. 55—0. 65, on the other hand, hT is 200 t m. On the basis of the equation, the calculation result of H is among 7. 7—9. 2 m. According to SPT and CPT results, the effective depth of the impact energy 2 000 kN • m in test zone approximates 7 m, which is less than the result based on the above specification, and meets with improvement requirements by using the impact energy 2 000 kN • m.

5 CONCLUSIONS

Based on the field observations and interpretation of the results presented, the following conclusions are drawn:

(1) The optimum number of drop is 4 and 5 when the impact energy level is respectively 2 000 kN • m and 1 500 kN • m.

(2) The influence depth of DC is approximately 7 m and 8 m when the impact energy level is respectively 1 500 kN • m and 2 000 kN • m.

(3) The radius of heave ranges from 7. 0 m to 7. 5 m when the impact energy level is 1 500 kN • m, and the radius of heave reaches 8 m when the impact energy level is 2 000 kN • m.

(4) The pore water pressure of foundation dissipates rapidly, and dissipates over during 3 h.

(5) By dynamic compaction methods with

silt materials in liquefiable soil areas, as tamper weight increases, the improvement extending to greater depths can be achieved.

(6) SPT and CPT are the powerful methods for investigating the effectiveness of ground improvement by DC.

(7) The impact energy 2 000 kN • m is recommended to remediate liquefiable silt soils, and it can eliminate the liquefaction potential of existing soils to depth of approximately 7 m from the ground surface.

References:

[1] Miao L C, Chen G, Hong Z S. Application of dynamic compaction in highway: A case study[J]. Geotech Geol Eng, 2006, 24(4):91-99.

[2] Zhang Lijuan, Li Zhangming, Han Jian. The application of dynamic-static drainage consolidation method on a silt ground disposal project [J]. Rock and Soil Mechanics, 2009, 30(2):567-571. (in Chinese)

[3] Kumar S. Reducing liquefaction potential using dynamic compaction and construction of stone columns [J]. Geotechnical and Geological Engineering, 2001, 19(2): 169-182.

[4] Adam D, Brandl H, Kopf F, et al. Heavy tamping integrated dynamic compaction control [J]. Ground Improv, 2007, 11(4):237-243.

[5] Cheng Ye, Gong Weiming, Dai Guoliang1, et al. Experimental study on time effect of wet drilling pile [J]. Transactions of Nanjing University of Aeronautics & Astronautics, 2008, 25(4): 311-317.

[6] Yu Xu, Zai Jinming, Zhuang Haiyang. Effects of soil-structure interaction on earthquake response of isolated structure system[J]. Journal of Nanjing University of Aeronautics & Astronautics, 2011, 43(6): 846-851. (in Chinese)

[7] Ma Chao, Wu Tieying. SPH-based numerical analysis for granular material model of sand and regolith[J]. Transactions of Nanjing University of Aeronautics & Astronautics, 2013, 30(1): 39-45.

[8] Nian Tingkai, Li Hongjiang, Yang Qing, et al. Research on improvement effect of high energy dynamic compaction (HEDC) under several complicated geological conditions[J]. Chinese Journal of Geotechnical Engineering, 2009, 31(1): 139-144. (in Chinese)

[9] Liu Jia, Luo Yan, Zhang Gongxin, et al. Experimental research on saturated mucky foundation treatment with well-point dewatering combined with dynamic compaction method[J]. Chinese Journal of Rock Mechanics and Engineering, 2009, 28(11): 2222-2227. (in Chinese)

[10] Feng S J, Shui W H, Gao LY, et al. Field studies of the effectiveness of dynamic compaction in coastal reclamation areas[J]. Bull Eng Geol Environ, 2010, 69(9):129-136.